Journal of Materials Science Research; Vol. 5, No. 1; 2016
ISSN 1927-0585 E-ISSN 1927-0593
Published by Canadian Center of Science and Education

Structure and Properties of Cast Iron DESIGNATED for Working Layer of Rolls

K. N. Vdovin[1], A. N. Zavalishchin[1], D. A. Gorlenko[1] & N. A. Feoktistov[1]

[1] FSBEI HBE Nosov Magnitogorsk State Technical University, Magnitogorsk, Russia

Correspondence: K. N. Vdovin, FSBEI HBE Nosov Magnitogorsk State Technical University, Magnitogorsk, Russia. E-mail: kn.vdovin@gmail.com

Received: October 23, 2015 Accepted: November 29, 2015 Online Published: December 29, 2015

doi:10.5539/jmsr.v5n1p77 URL: http://dx.doi.org/10.5539/jmsr.v5n1p77

Abstract

The formation of the structure and properties of cast irons designated for the working layer during solidification and subsequent tempering of Indefinite Chill Double Poured Centrifugal Casting Rolls (ICDP) has been studied.

Graphitization of cast irons designated for the working layer of rolls occurs under isothermal conditions at high temperatures, which vary over the cross section and resulted from casting the roll core. At subsequent slow cooling, secondary carbides precipitate and austenite partially transforms into martensite; the resulting end structure consists of martensite and austenite metallic base (primary austenite dendrites) with 11.4 per cent of retained austenite, 26 per cent of eutectic and secondary carbides, and 2.6 per cent of flake graphite.

The amount of retained austenite in the metallic base of the cast structure of cast iron designated for the working layer, heated to 430 °C, decreases from 11.4 per cent to 3.2 per cent due to the partial transformation into bainite. The martensite tetragonality decreases due to the carbide precipitation; the existing excess phases grow and the new ones are formed; the total volume fraction of the carbide phase increases to 29.8 per cent and graphite to 3.7 per cent.

Keywords: Roll, cast iron, solidification, tempering, microstructure, martensite, retained austenite, carbides, graphite

1. Introduction

The improvement of the rolled products quality and production efficiency is one of the most important tasks for the metallurgical sector under fierce competition on the rolled products market. Rolls, the key tool of rolling-mill machinery, are significant in the solution of these tasks with the expenses of 15 ... 20 per cent in the cost structure of rolled products, moreover, their durability has considerable impact on the metal product quality and steel mill productivity (Traino 2008). More severe operating conditions of modern hot-rolling mills cause a significant increase in the requirements for the roll barrel surface, its axial part and trunnions (Ray et al., 2000).

Centrifugally cast iron rolls meet these requirements best of all due to the absence of the transition zone from the core to the working layer, made of high-alloy cast iron, which is characterized by a homogeneous structure and has higher density, strength, and ductility, as well as keeps its hardness unchanged throughout the entire operating period that results in the constant level of roll wear resistance (Martini & Gostev, 1999; Ray, Prasad, Barhai, & Mukherjee, 2004; Sinha, Indimath, Mukhopadhyay, & Bhattacharyya, 2014; Martini, 1999). Rolls made of high chrome cast iron (Hi-Cr) are installed in the first three stands of the finishing group, and rolls made of indefinite (mottled) ICDP iron are installed in the last three stands (Gostev, 2008; Palit, Jugade, Jha, Das, & Mukhopadhyay, 2015). The working layer made of the Ni-Cr white iron that contains the martensite, eutectic and secondary carbides, retained austenite, and graphite can help to achieve the high quality of the work rolls for the last finishing stands of rolling mills (Asensio-Lozano & Álvarez-Antolín, 2008).

Carbides, metallic base, and graphite are the main structural constituents of wear-resistant mottled cast irons.

The carbide phase in cast iron is determinative for the abrasive wear processes and the wear resistance coefficient. The wear resistance coefficient depends on the amount of carbides and the increased size of carbide inclusions decreases wear resistance of cast irons (Kang, Suh, Oh, & Lee, 2014).

The degree of influence of carbide sizes depends on the conditions and nature of abrasive wear. This is associated with the stress distribution between the carbide and metallic base: large carbide inclusions, especially in a soft matrix, crack and crumble under stresses, generated by an abrasive particle; small carbide inclusions transfer some portion of the stresses to the metallic base and they do not crumble (Ray, Mukherjee, Sarkar, & Mishra, 1994; Lee, Kim, Ryu, & Shin, 1997; Nilsson & Olsson, 2013). The high wear resistance of iron with the most suitable carbide structure is feasible only when the metallic base itself has a high degree of microhardness, provides strong carbide fixation, and is not undergone deformation when loading in operation. The sizes of the base areas between carbides should be sufficiently small in order to minimize the selective abrasive wear of the base, carbide denudation, their washout, or breaking off. Martensite and retained austenite, unstable under these wear conditions, meet these requirements to the greatest extent but a ferrite, soft, pearlite or stable austenitic metallic base is less suitable.

The metallic base of cast iron designated for the working layer, as well as the carbide phase, influences on the forming roll resistance. At the same characteristics of the carbide constituent, wear resistance is linearly dependent on microhardness of the base and is independent of its phase composition. Thus, martensite is the best base metal in order to obtain maximum wear resistance (Al-Rubaie & Pohl, 2014; Jinzhu, Shizhuo, & Yongfa, 1993).

The influence of the graphite, contained in the structure of mottled cast irons, on wear resistance of rolls may be both positive and negative and depends on the shape and number of inclusions, as well as the working conditions.

A negative impact should be noted that graphite possesses poor resistance to extension and shearing, consequently, graphite inclusions are unable to carry heavy loads. Uneven distribution of graphite inclusions decreases all mechanical properties of cast iron and influences on its fatigue strength, but the growth of graphite inclusions and the decreased shape of graphite inclusions increase the micro defects and degree of wear.

The positive impact of graphite on the wear resistance of rolls is more prevalent due to the following advantages: the places of occurrence of spherical graphite are lubricant reservoirs; large graphite inclusions absorb solid abrasive particles; increased thermal conductivity of cast iron; improved kinetics of the oxide film formation on the surface of rolls; increased thermal wear resistance. The occurrence of thermal fatigue cracks and graphite precipitation promotes oxidation of the structural constituents of cast iron, and under the influence of the friction forces in the zone of deformation it causes the separation of cementite particles, but thanks to the graphite this process does not spread in depth. The thermal endurance of cast iron with evenly distributed graphite is 40 ... 100 per cent more than the thermal endurance of cast iron with graphite concentration in the form of nests and sockets, and finely crushed inclusions provide a minimum tendency to heat checking (Kuskov, 2006; Asensio-Lozano, Álvarez-Antolín, & Vander Voort, 2008).

The purpose of this work is to study the structure and properties of cast iron designated for the working layer of rolls in as - cast state and after tempering at 430° C.

2. Methods of Carrying out Research

Cast iron indefinite (mottled) rolls are produced by centrifugal casting method, and two electric furnaces (induction and electric) are used to smelt metal for their production at Magnitogorsk Rolls Plant JSC. A centrifugal machine is used to cast the surface work layer of the roll of alloyed cast iron, and the core of the roll is poured into a special caisson hole to form a core of grey cast iron, the upper and lower necks.

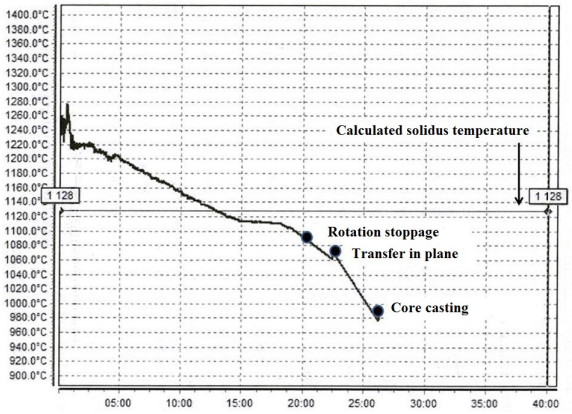

Figure 1. Changes in the temperature of cast iron designated for the working layer after casting into a chill before pouring the core, optical pyrometer data

The temperature and time required for the necessary operations are under control in the process of roll manufacturing. Platinum - rhodium / platinum thermocouples measure the temperature changing of melted irons, and a special optical pyrometer measures the temperature of the interior surface of iron, which is in the mould of a centrifugal machine. The data obtained using this pyrometer is formed a diagram of temperature changing of iron during crystallization of the working layer of the roll (Figure 1).

The chemical composition of the experimental cast iron, shown in Table 1, was analysed by spectral methods using the spectrometers: OBLF QSN 750 (GOST 18895-97) and OBLF GS 1000 (GOST 27611-88).

Table 1. Chemical composition of cast iron designated for the working layer

C	Si	Mn	S	P	Cr	Ni	V	Ti	Nb	Cu
3.00-3.20	0.7-1.0	0.75-0.95	0.015	0.045	1.5-1.85	4.0-4.6	0.15-0.2	0.01-0.02	0.45-0.70	0.11-0.12

The microstructure was examined using the optical microscope Meiji-2700 at 50- to 1000-fold magnification and a computer system of images analysis Thixomet Standard PRO. Marble's Reagent (50 ml HCl, 2 g $CuSO_4$, 50 ml C_2H_5OH, 50 ml H_2O) was applied for revealing the microstructure of the cast iron samples under investigation that allowed the boundaries of the various structural constituents to be clearly defined.

X-ray diffractometer DRON-3 was used for X-ray phase analysis of the total X-ray spectrum of cast iron at a voltage of 32 kV and a current of 10 mA with Mo – k_α radiation; on the potentiometer operable in the record mode, and automatic memory on the PC with the help of the program package DIFWIN1 (step scanning mode: step shooting of 0,05 º (in the scale of 2Θ), the exposure time of 10 sec., angles within a range of 10 to 40º).

The amount of retained austenite was calculated from the formula:

$$K_A = \frac{1 - K_K}{1 + \frac{F_{пр}}{F_A} * \frac{\Psi_A}{\Psi_{пр}} * \frac{P_{(HKL)A}}{P_{(HKL)np}} * \frac{V_{np}}{V_A} * \frac{S_A^2}{S_{np}^2} * \frac{\sin^2\Theta_A}{\sin^2\Theta_{np}}} \quad , \qquad (1)$$

where Ψ is an angular factor of the diffraction peak in polycrystalline samples;

$P_{(HKL)}$ is the factor for recurrence of planes with Miller indices (HKL);

$V_i=a^3$ is the volume of the unit cell in angstroms;

S^2_i is a structural factor: for the body-centered cubic lattice is 4, for the face-centered cubic lattice is 16;

$Sin^2\Theta_i$ is squared half the Bragg angle.

The interference lines {112} recorded for α-Fe (Θ=17º40') and the interference lines {113} recorded for γ-Fe (19º07') are planimetrically measured and limited areas F_A and $F_{пр}$ are determined with the use of the program package DIFWIN1.

The amount of martensite is determined from the equation:

$$K_A + K_{пр} + K_к = 1, \qquad (2)$$

where K_A, $K_{пр}$, $K_к$ are the volume fractions of retained austenite, the decomposition products of austenite and carbides, respectively.

The chemical composition of the phases was analysed by X-ray spectrum method using scanning electron microscopes (SEM) TESCAN VEGA II XMU (Czech Republic) equipped with an INCA energy-dispersive X-ray microanalysis system (EDS) ENERGY 450, with a detector of OXFORD (UK) and a software package of INCA (Ekaterinburg), as well as SEM of JEOL, the model JSM-6490LV in the laboratory of NMSTU (Magnitogorsk, Russia).

A dilatometric method was used to study the start and end temperatures of phase transitions in the sample of cast iron designated for the working layer, followed by a change in the specific volume. Investigations were carried out on a Gleeble 3500, the sample is heated by direct passing a current through the vacuum.

The method of computer simulation with the help of a licensed software LWMFlow 4.2r2 was used to analyse thermal processes occurring in the body of the solidifying casting.

3. Research Results and Discussion

The research study found that crystallization of the working layer of alloyed cast iron starts at 1234 ° C in a rotating chill under the effect of centrifugal force due to the heat removal through the mould walls.

The intensity of heat removal varies with time and is dependent on the thickness of the solidified metal, which in turn affects the size of the dendrites. Randomly oriented primary austenite dendrites are crystallized directly in a thin surface layer. Due to centrifugal force elongated columnar crystals, formed forth and oriented in a direction perpendicular to the mould cavity wall at ordinary crystallization, lose stability relatively to the direction of heat removal and become oriented perpendicular to this direction (Figure 2).

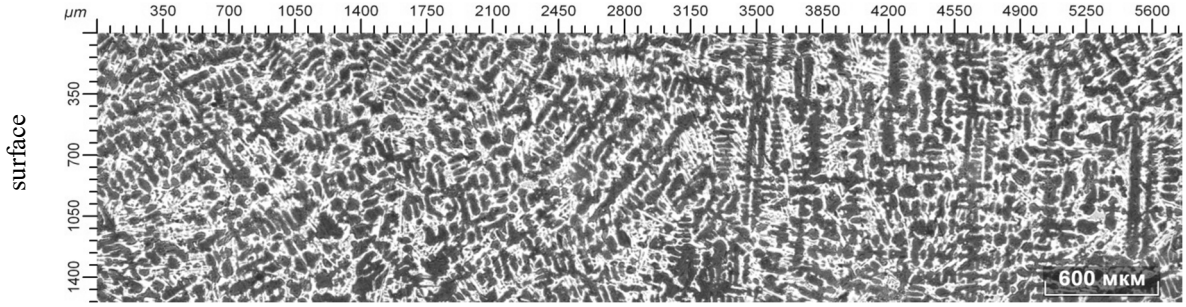

Figure 2. Panoramic image of the microstructure of cast iron designated for the working layer

After the separation of primary austenite dendrites from the liquid phase crystallization ends in the formation of eutectics (Figure 3) at a temperature of 1118 ° C, corresponding to the horizontal portion of the cooling curve of cast iron designated for the working layer (Figure 1). For crystallization under these conditions, it was possible to achieve 10 ° C of supercooling and 1128 ° C of the solidus temperature.

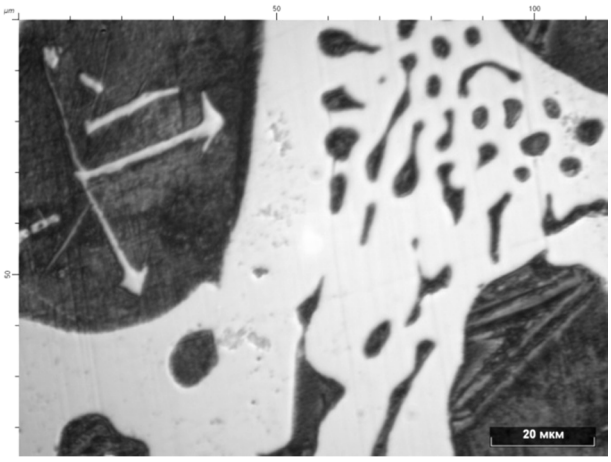

Figure 3. Eutectic in cast iron designated for the working layer

After the temperature of the crystallized working layer reduced to 980 ... 1000 ° C (Figure 1) a chill is transferred to the caisson by a crane and mounted in the moulding box of the lower roll neck. The mould of the upper roll neck is installed on the chill, as well as the funnel for pouring iron into the core at temperature of 1370 ... 1380 ° C; as a result, the working layer of alloyed cast iron is heated and partially melted. Since an optical pyrometer is unfit for a further determination of the change in the temperatures of the working layer, theoretical calculations of the temperature fields in the cross section of the roll in the casting mould at different times, obtained with the help of LVMFlow program, were used (Figure 4).

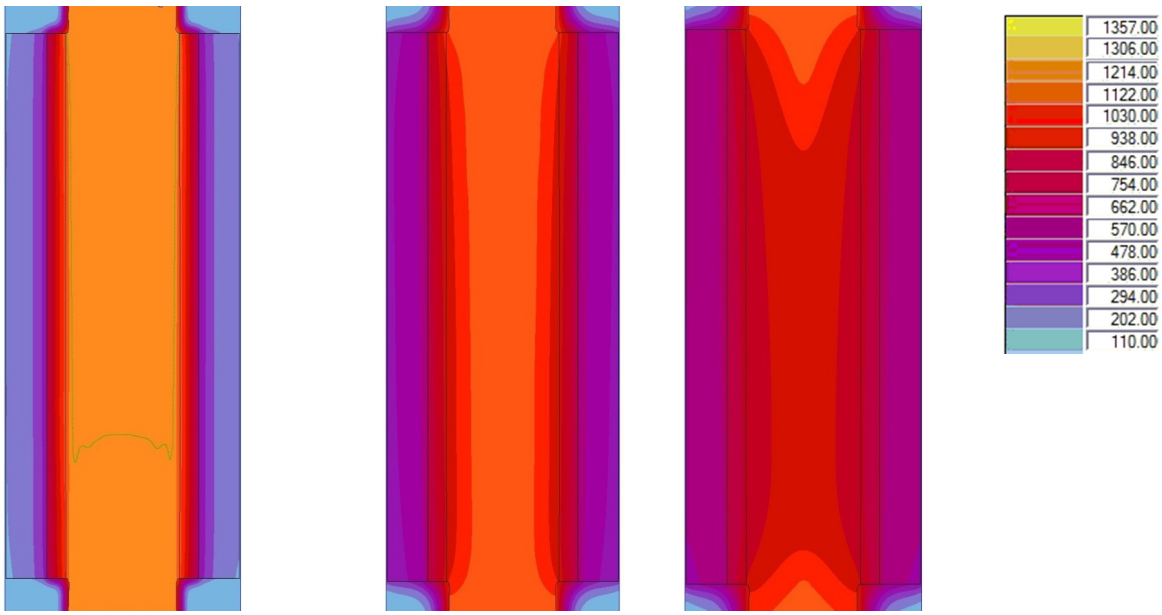

Figure 4. Graphical representation of the temperature distribution over the cross section of the roll: a - in18 minutes; b - in 105 minutes; c - in 196 min; d - colour-grade matching to temperature, ° C

Temperatures in the fusion area of the working layer with the core, the centre and the surface of the working layer, defined by calculation, are shown in Figure 5. According to the calculations, the working layer of cast iron for a long time is under isothermal conditions at high temperatures, which vary from the layer thickness, resulted from the roll core pouring, that causes partial decomposition of carbides existing in the structure with the release of carbon in the form of flake graphite (Figures 6, 7).

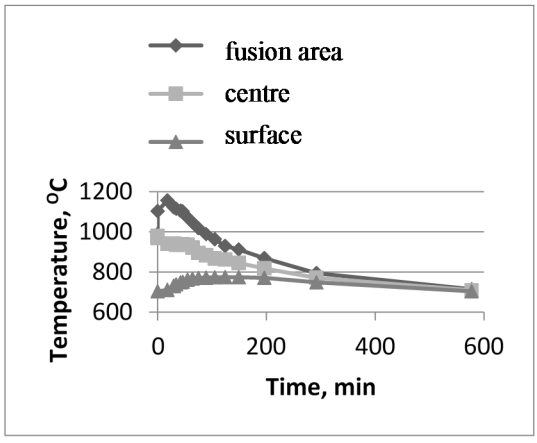

Figure 5. Changes in the temperature of the working layer zones after pouring the core

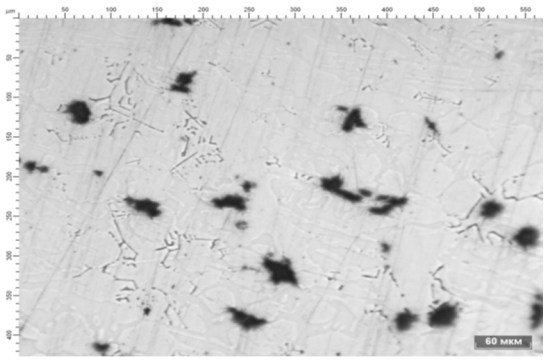

Figure 6. Microstructure of iron designated for the working layer after cooling with isothermal holding: large dark inclusions - graphite; thin dark inclusions - secondary carbides (not pickled)

The carbon solubility decreases during cooling after crystallization throughout the whole temperature range and the secondary carbides of various shapes precipitate from the metallic base, as well as the flake graphite precipitation is continuing.

The structure of iron designated for the working layer, cooled without being isothermally hold, in which there are no graphite inclusions proves out that the partial graphitization of iron cementite designated for the working layer

is the result of isothermal holding. When cooling the excess phase precipitates only in the form of secondary carbides (Figure 8).

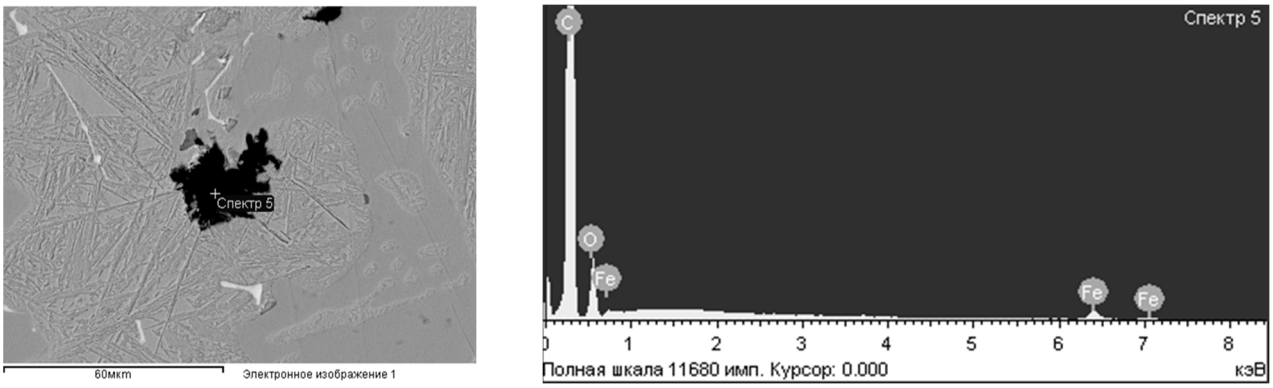

a b

Figure 7. The electron image (a) and spectrum of graphite inclusions (b)

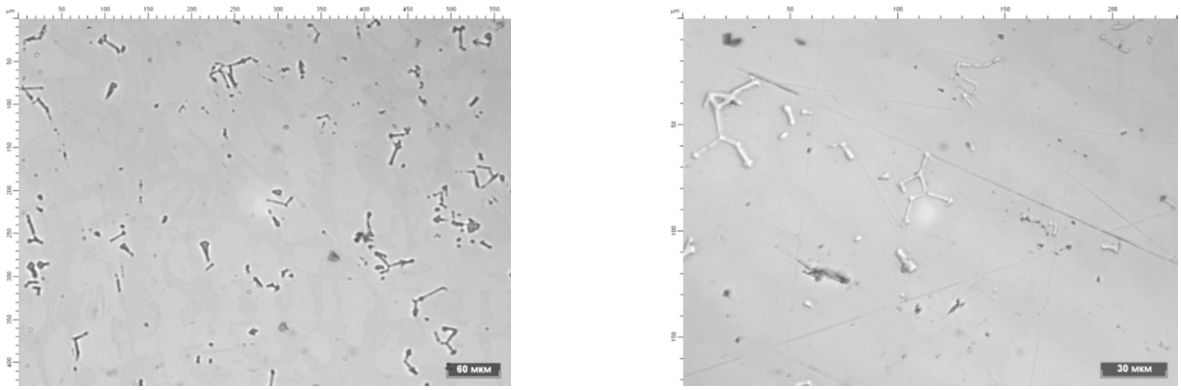

Figure 8. Microstructure of iron designated for the working layer after cooling without isothermal holding: thin inclusions - secondary carbides, (not pickled)

The formation of the structure of iron designated for the working layer in the process of roll manufacturing of grade LPHNd-71 ends with the partial transformation of austenite into martensite when a martensite start temperature is 180 ° C (Figure 9).

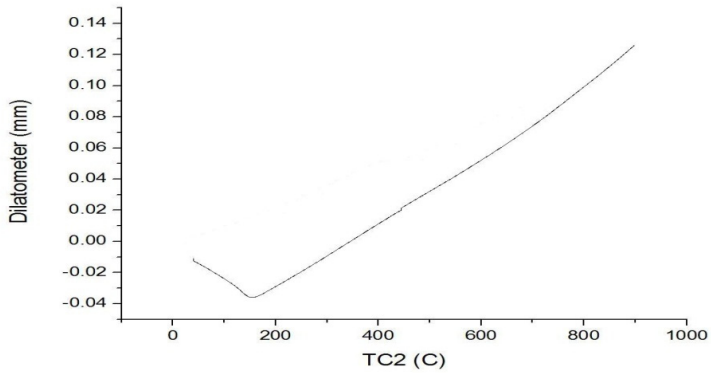

Figure 9. Dilatometric curve of cast iron designated for the working layer obtained in cooling at a rate of 5 ° C / min

Thus, it was found that the final structure of cast iron designated for the working layer consists of the martensite-austenite metallic base (primary austenite dendrites), eutectic carbides, and excess phases in the form of secondary carbides and graphite inclusions (Figure 10).

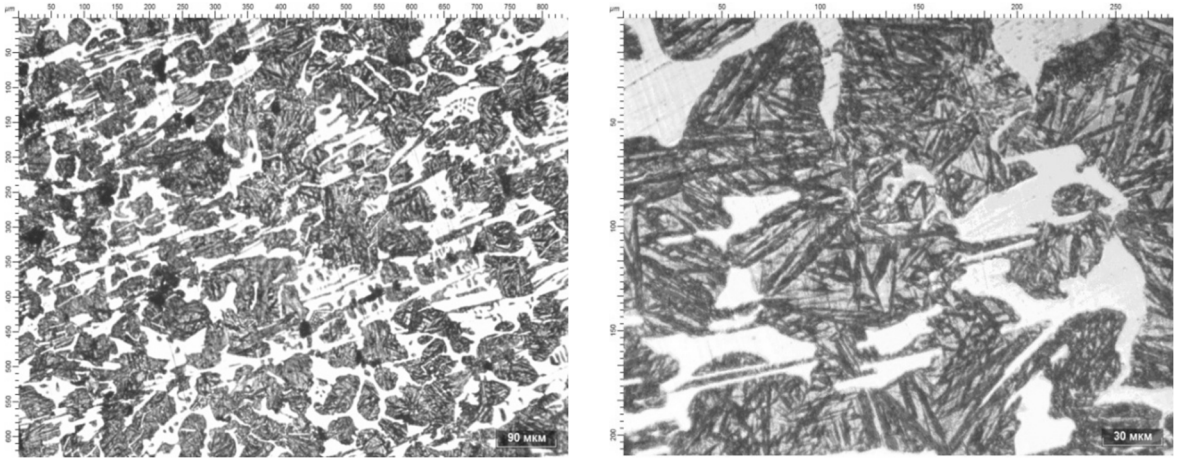

Figure 10. Microstructure of cast iron designated for the working layer in as-cast state

The amount of martensite and retained austenite was determined with the help of X-ray structural analysis; their content in the metallic base is equal to 60.0 per cent and 11.4 per cent, respectively.

The size of the martensite needles was defined in cast iron designated for the working layer, which ranges from a long size of grade 9, growing through the former austenite dendrite, to a short size of grade 7, growing in the former austenite dendrite at an angle to the existing needles.

The analysis of the diffractogram allowed one to determine that the martensite formation results in a tetragonal splitting of distinctive maximum of α-iron (2.01 Å) and its shift towards larger interplanar distances – 2.029 Å (Figure 12).

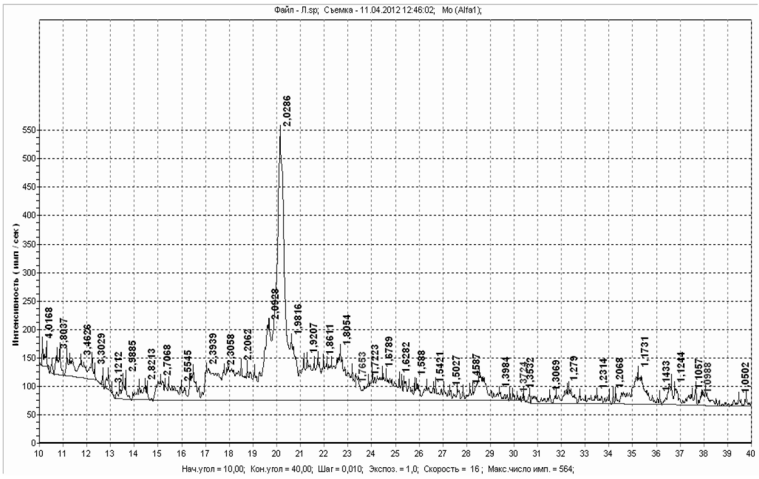

Figure 12. Diffractogram of iron designated for the working layer in as-cast state

Shifting is caused by the occurrence of double peak in the martensite lattice: the left one corresponds to the diffraction from the crystal plane (011), the right one corresponds to the diffraction from the plane (110); herewith the intensity at the maxima, forming this pair, is not the same as the repeatability multiplication factor for these planes is 8 and 4, respectively (Figure 13). Having determined the periods "a" and "c", we calculated the degree of the tetragonal martensite c / a = 1.069, a decrease in the value of which gives evidence of the martensite decay.

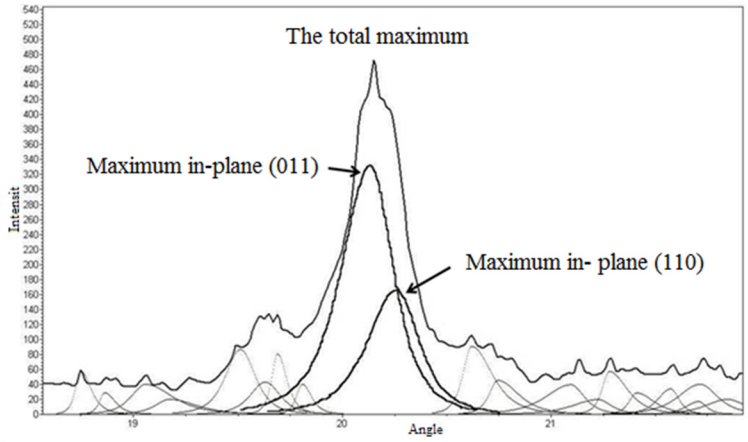

Figure 13. A fragment of diffractogram of cast iron designated for the working layer in as - cast state: distinctive maximum of α-iron with martensitic splitting

The volume fraction, the average area, and the density of the distribution of graphite and carbides were determined by metallographic analysis method. The hardness of iron designated for the working layer, and the average microhardness of the base and carbides were determined. Data obtained by metallographic analysis and mechanical test results of cast iron designated for the working layer in as - cast state are represented in Tables 2 and 3.

The working layer of the roll while in operation undergoes thermal loads related to heating during the contact with the rolled strip and subsequent water cooling, resulting in austenite disintegration in cast iron designated for the working layer, the amount of which in as-cast state is more than 11 per cent with the martensite formation. This process results in the occurrence of stresses, cracks on the roll surface and with its subsequent spalling. To reduce the amount of retained austenite and relieve stresses, which arise during the formation of its degradation products, rolls are subjected to tempering with slow heating to 430 ° C.

Table 2. Data obtained by metallographic analysis

Volume fraction of carbides, %	26
The average area of carbides, mkm^2	146
The density of distribution of carbides, 1 / mm^2	1783
Volume fraction of graphite inclusions, %	2,6
The average size of graphite inclusions, mkm^2	125
The density of distribution of graphite inclusions, 1 / mm^2	235

Table 3. The test results on the hardness and microhardness

Hardness, HRC	52,5
The average microhardness of the base, HV	497
The average microhardness of carbides, HV	942

This processing resulted in the cast iron structure, which consists of the metallic base, formed by the needle phases and retained austenite, eutectic and secondary carbides and graphite (Figure 14).

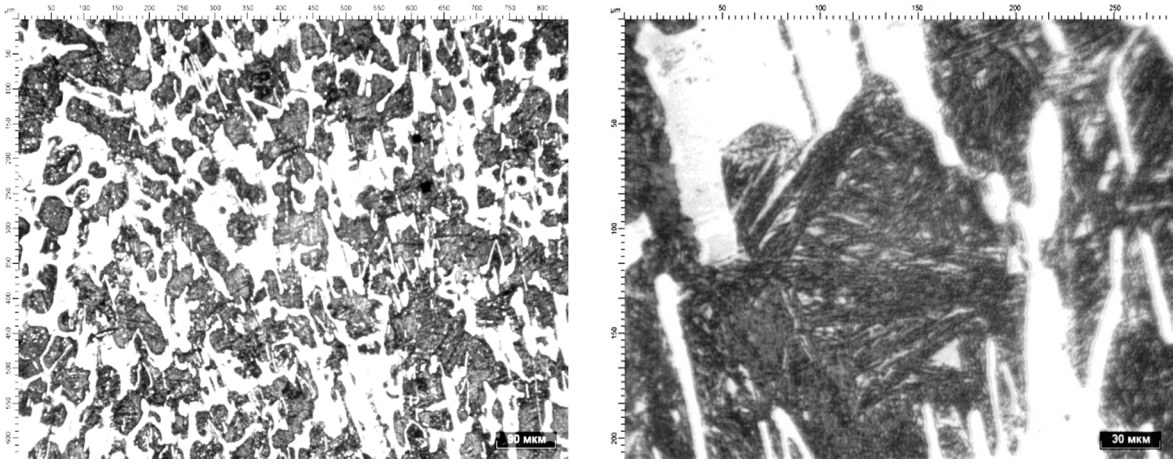

Figure 14. Microstructure of iron designated for the working layer after tempering at 430 ° C

Qualitatively, the structure of iron designated for the working layer after tempering at 430°C is not different from the structure of iron in the as-cast state. The difference can be observed for the quantitative relationships of the phases (Vdovin, Gorlenko, & Zavalishchin, 2013).

Tempering results in an increase in the size of excess phases, precipitated during cooling after solidification, and the formation of new additional secondary carbides and graphite inclusions in the martensitic-austenitic metallic base. At the same time, austenite, impoverished in alloying elements due to the excess phase release during heating, becomes less stable to the disintegration, and is partially transformed to bainite during cooling, which together with the tempered martensite is included in the composition of the acicular structure of the metallic base.

Using X-ray diffraction analysis we determined that the amount of retained austenite is reduced from 11.4 per cent in the as-cast state to 3.0 ... 3.2 per cent after tempering. Heating to 430°C decreases the shifting of α-iron specific peak to values of 2.015 Å, compared with a cast state (2,028 Å) (Figure 15).

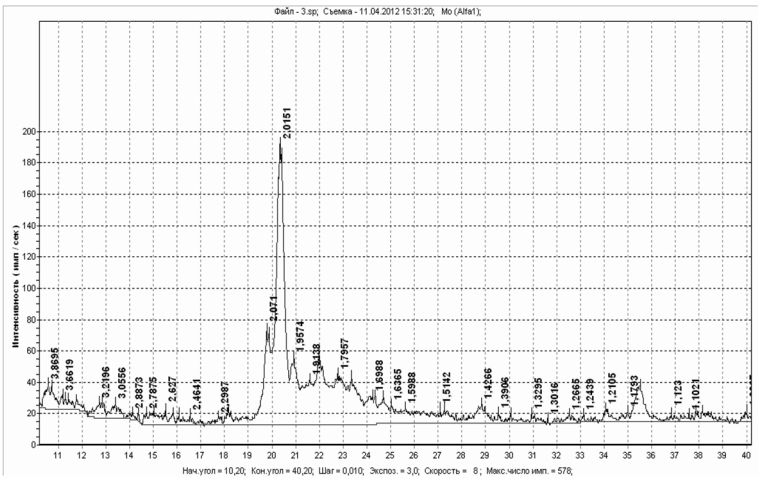

Figure 15. Diffractogram of cast iron designated for the working layer after tempering at 430 ° C

As a result of martensite desintegration the ratio of the axes of its tetragonal lattice relative to the as-cast state decreases, and the tetragonal degree c/a reduces from 1,069 to 1,013, correspondingly (Figure 16).

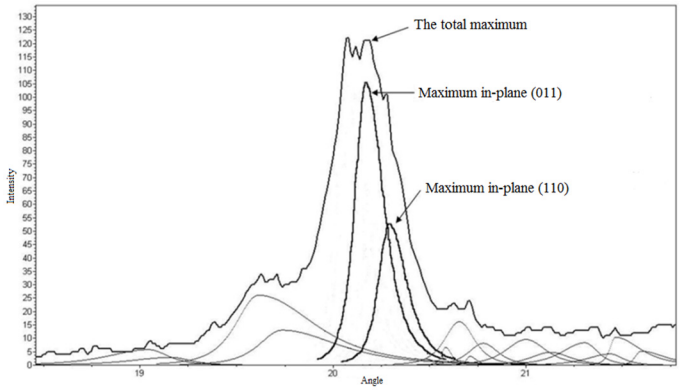

Figure 16. A fragment of diffractogram of iron designated for the working layer after tempering at 430 ° C:distinctive maximum of α-iron with martensitic splitting

In addition to reducing the amount of retained austenite, changes occur in the volume fraction, the number of impurities per unit area, and the average area of excess phases after heating cast iron designated for the working layer to 430 ° C (Vdovin, Gorlenko, & Zavalischin, 2013). The volume fraction of graphite increases more than 1 per cent, and becomes equal to 3.7 per cent (2.6 per cent in as-cast). The number of graphite impurities per unit area increases more than twice, and the average area of inclusions decreases due to the fact, that the precipitated graphite particles are less than "as-cast" (Figure 17).

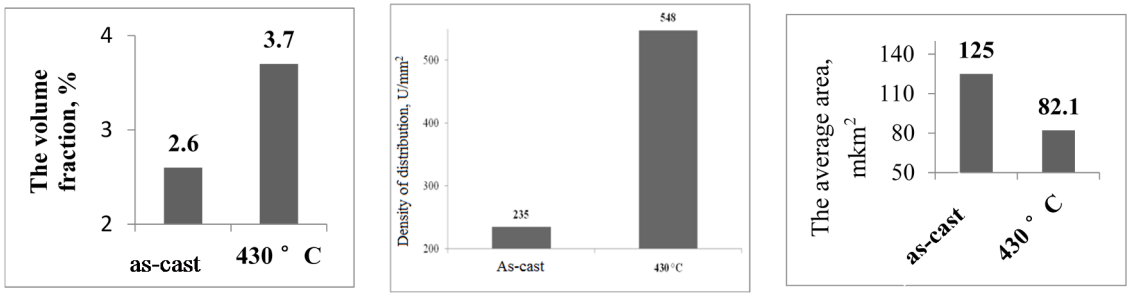

a b c

Figure 17. Characteristics of graphite inclusions: a - the volume fraction, %; b - the density of distribution, units / mm^2; c - the average area, mkm^2

The total volume fraction of eutectic and secondary carbides increases from 26 to 29.8 per cent, the number of inclusions per unit area increases almost twice from 1783 units / mm^2 to 3181 units / mm^2, herewith, the amount of eutectic carbides does not changed. The increase in the total volume fraction of the carbide phase occurs due to the additional extraction of dispersed secondary carbides, which also results in a decrease in values of the average area of the carbide phase (Figure 18).

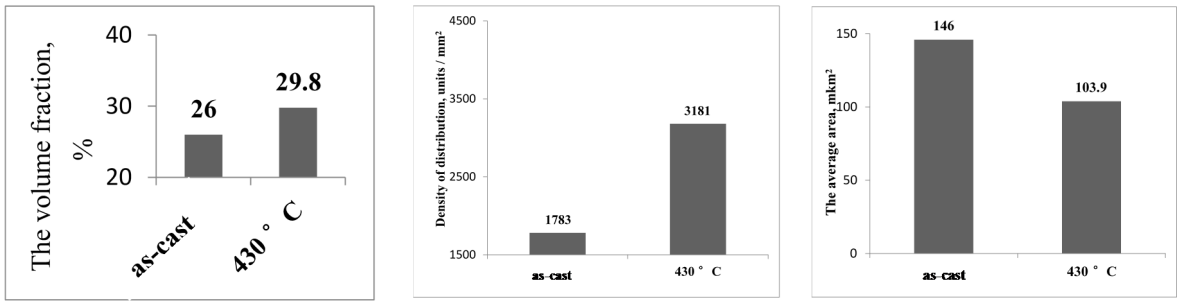

a b c

Figure 18. Characteristics of the carbide phases: a - the volume fraction, %; b - the density of distribution, units / mm^2; c - the average area, mkm^2

The average microhardness of the metallic base and carbides, as well as hardness in general of iron designated for the working layer after tempering at 430 ° C remain practically unchanged. Two processes of changes in hardness, which compensate each other, occur in the metallic base: decreasing the number of retained austenite increases microhardness, and the disintegration of martensite reduces microhardness (Figure 19 a). Microhardness of the carbide phase does not change for the newly precipitated excess carbides have the same microhardness as "as-cast" (Figure 19 b). The precipitation of solid secondary carbides and soft graphite and bainite does not result in the change of hardness in iron after tempering at a temperature 430ºC as a whole (Figure 19).

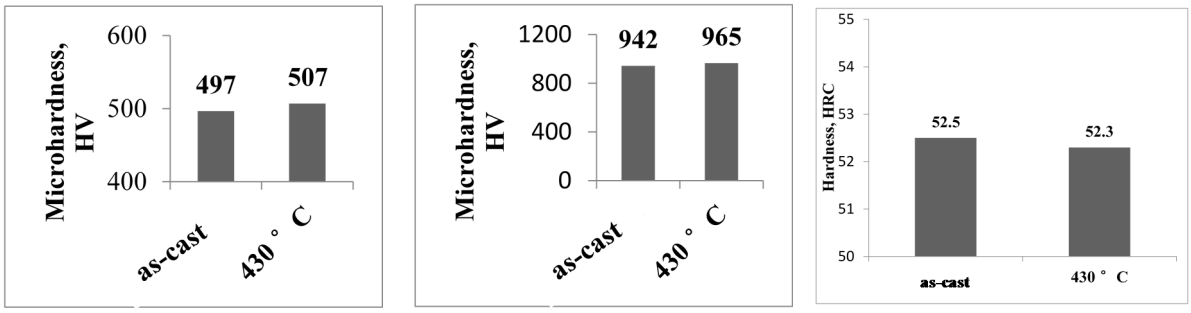

a b c

Figure 19. Mechanical properties after tempering at 430 ° C: a - the average microhardness of the metallic base, HV; b - the average microhardness of carbides, HV; c - hardness, HRC

4. Conclusions

The following conclusions have emerged from the present study.

The microstructure of cast iron designated for the working layer, which consists of 60 per cent of martensite, 11.4 per cent of retained austenite, 26 per cent of eutectic and secondary carbides, 2.6 per cent of graphite, is formed during crystallization and further cooling with further isothermal holding.

Partial graphitization of cast iron cementite designated for the working layer is a result of isothermal holding, in the case of its absence while cooling the excess phase precipitates only in the form of secondary carbides.

Cast iron tempering at a temperature of 430°C changes the quantitative phase relationship relative to the as-cast state, herewith the structure consists of 63.4 per cent of martensite, 3.1 per cent of retained austenite, 29.8 per cent of eutectic and secondary carbides, and 3.7 per cent of graphite.

References

Al-Rubaie, K. S., & Pohl, M. (2014). Heat treatment and two-body abrasion of Ni-Hard 4. *Wear*, *312*(1), 21-28.

Asensio-Lozano, J., & Álvarez-Antolín, J. F. (2008). Saturated fractional design of experiments: Toughness and graphite phase optimizing in Nihard cast irons. *Journal of Materials Engineering and Performance*, *17*(2), 216-223. DOI 10.1007/s11665-007-9138-8.

Asensio-Lozano, J., Álvarez-Antolín, J. F., & Vander Voort, G. F. (2008). Identification and quantification of active manufacturing factors for graphite formation in centrifugally cast Nihard cast irons. *journal of materials processing technology*, *206*(1), 202-215. DOI:10.1016/j.jmatprotec.2007.12.015.

Gostev, K. A. (2008). Heat treatment in the production of cast rolls. *Steel, 9*, 79-84.

Jinzhu, L., Shizhuo, L., & Yongfa, M. (1993). Wear resistance of Ni-hard 4 and high-chromium cast iron re-evaluated. *Wear*, *166*(1), 37-40.

Kang, M., Suh, Y., Oh, Y. J., & Lee, Y. K. (2014). The effects of vanadium on the microstructure and wear resistance of centrifugally cast Ni-hard rolls. *Journal of Alloys and Compounds*, *609*, 25-32.

Kuskov, Y. M. (2006). Influence of graphite inclusions on the durability of the cast and hardfaced hot rolling rolls. *Steel, 2*.

Lee, S., Kim, D. H., Ryu, J. H., & Shin, K. (1997). Correlation of microstructure and thermal fatigue property of three work rolls. *Metallurgical and materials transactions A*, *28*(12), 2595-2608. DOI 10.1007/s11661-997-0017-6.

Martini, F. (1999). Main manufacturing and service requirements for the backup rolls and work rolls of modern hot-strip mills. *Metallurgist*, *43*(8), 365-370. DOI 10.1007/BF02463657

Martini, F., & Gostev, K. A. (1999). New generation of wear-resistant bimetallic rolls for sheet mills. *Metallurgist*, *43*(5), 200-204.

Nilsson, M., & Olsson, M. (2013). Microstructural, mechanical and tribological characterisation of roll materials for the finishing stands of the hot strip mill for steel rolling. *Wear*, *307*(1), 209-217. DOI: 10.1016/j.wear.2013.09.002.

Palit, P., Jugade, H. R., Jha, A. K., Das, S., & Mukhopadhyay, G. (2015). Failure analysis of work rolls of a thin hot strip mill. *Case Studies in Engineering Failure Analysis*, *3*, 39-45. DOI:10.1016/j.csefa.2015.01.001.

Ray, A., Mukherjee, D., Sarkar, B., & Mishra, S. (1994). Influence of microstructure on the premature failure of a second-intermediate Sendzimir mill drive roll. *Journal of materials engineering and performance*, *3*(5), 649-656. DOI 10.1007/BF02645263.

Ray, A., Prasad, M. S., Barhai, P. K., & Mukherjee, S. K. (2004). Metallurgical investigation of prematurely failed hot-strip mill work-rolls: some microstructural observations. *Journal of Failure Analysis and Prevention*, *4*(3), 58-66. DOI 10.1007/s11668-996-0016-8.

Ray, A., Prasad, M. S., Dhua, S. K., Sen, S. K., & Jha, S. (2000). Microstructural features of prematurely failed hot-strip mill work rolls: Some studies in spalling propensity. *Journal of materials engineering and performance*, *9*(4), 449-456. DOI 10.1361/105994900770345854.

Sinha, P., Indimath, S. S., Mukhopadhyay, G., & Bhattacharyya, S. (2014). Failure of a Work Roll of a Thin Strip Rolling Mill: A Case Study. *Procedia Engineering*, *86*, 940-948. DOI:10.1016/j.proeng.2014.11.117

Traino, A. I. (2008). Rational roller operation and restoration. *Steel in Translation*, *38*(10), 871-875.

Vdovin, K. N., Gorlenko, D. A., & Zavalischin, A. N. (2013). Structure changes of chromium-nickel indefinite cast irons in heating. *Vestnik of Nosov Magnitogorsk State Technical University, 5*(45), 9-11.

Vdovin, K. N., Gorlenko, D. A., & Zavalishchin, A. N. (2013). Influence of industrial tempering on the composition of complex cast iron. *Steel in Translation*, *43*(5), 288-290.